molecules

MDPI

*Article*

# Determination of Phosphate as an Ion-Association Complex of 11-Molybdovanadophosphate and Diindodicarbocyanine Based on Selective Oxidation of Excess Dye

**Andriy B. Vishnikin [1,2,*], Svitlana V. Khlyntseva [1,2], Yaroslav Bazel [1,*], Ioseph Balogh [3] and Ihor E. Barchiy [4]**

[1] Department of Analytical Chemistry, P.J. Šafárik University in Košice, 04154 Košice, Slovakia; khlyntseva@yahoo.com
[2] Department of Analytical Chemistry, Dnipro National University, 49050 Dnipro, Ukraine
[3] Department of Chemistry, University of Nyíregyháza, 4400 Nyíregyháza, Hungary; baloghj29@gmail.com
[4] Department of Inorganic Chemistry, Uzhhorod National University, 88000 Uzhhorod, Ukraine; igor.barchiy@uzhnu.edu.ua
* Correspondence: andrii.vyshnikin@upjs.sk (A.B.V.); yaroslav.bazel@upjs.sk (Y.B.)

**Abstract:** The elimination of absorbance of excess dye by selective oxidation was first proposed for analytical methods using the formation of ion-association complexes (IAs). On this basis, a new sensitive and selective spectrophotometric method for the determination of phosphate in the form of the IA of 11-molybdovanadophosphate with diindodicarbocyanine (DIDC) was developed. Symmetric diindodicarbocyanine and diindotricarbocyanine dyes can be completely oxidized by sufficiently strong oxidizing agents such as permanganate, dichromate, cerium (IV), and vanadate. Of the three dyes investigated (DIDC, N,N′-dipropyldiindodicarbocyanine, and diindotricarbocyanine), the best results were obtained with DIDC. A mixture of molybdate, vanadate, and nitric acid was preferably used as an oxidizing agent. Selective decolorization of only free dye ions, as well as changes in the IA spectrum compared to the dye spectrum, were explained by the isolation of the dye due to the formation of poorly soluble IA nanoparticles and changes in the redox potential of the dye due to its aggregation. The following optimal conditions for phosphate determination were found: 0.3 M nitric acid, 0.43 mM sodium molybdate, 0.041 mM sodium vanadate, 0.015 mM DIDC, and 18 min for the reaction time. The molar absorptivity of the IA was $1.86 \times 10^5$ $mol^{-1} \cdot L \cdot cm^{-1}$ at 600 nm, and the detection limit for phosphate was 0.013 μM. The developed method was applied to the determination of phosphate in natural water samples.

**Keywords:** phosphate determination; polymethine dye oxidation; ion association complex; 11-molybdovanadophosphate; spectrophotometry

check for updates

Academic Editor: Evagelos Gikas

Received: 9 March 2025
Revised: 18 April 2025
Accepted: 21 April 2025
Published: 22 April 2025

**Citation:** Vishnikin, A.B.; Khlyntseva, S.V.; Bazel, Y.; Balogh, I.; Barchiy, I.E. Determination of Phosphate as an Ion-Association Complex of 11-Molybdovanadophosphate and Diindodicarbocyanine Based on Selective Oxidation of Excess Dye. *Molecules* **2025**, *30*, 1872. https://doi.org/10.3390/molecules30091872

**Copyright:** © 2025 by the authors. Licensee MDPI, Basel, Switzerland. This article is an open access article distributed under the terms and conditions of the Creative Commons Attribution (CC BY) license (https://creativecommons.org/licenses/by/4.0/).

## 1. Introduction

Phosphate is an essential substance for the growth and reproduction of living organisms and is a major factor in the characterization of rivers, lakes, and oceans [1–3]. A significant excess of the natural content of total phosphorus (>0.02 mg $L^{-1}$) stimulates the growth of photosynthetic aquatic micro- and macroorganisms in undesirable amounts, which in turn leads to eutrophication of the water bodies and possibly to changes in the structure and functions of freshwater and marine ecosystems [4]. Several recent reviews provide a comprehensive overview of analytical methods for the determination of phosphate [1,5–10].

Spectrophotometric methods based on the reduction of the 12-molybdophosphate heteropolyanion (HPA) $PMo_{12}O_{40}^{3-}$ (12-MPA) are most commonly used for the determination of orthophosphate [8,11–13]. The method exists in several variants, differing in the reducing agent used, acidity, and temperature. Standard spectrophotometric heteropolyblue-based procedures for phosphate determination have an LOD of about 10 μg $L^{-1}$. This LOD is inadequate for the determination of dissolved reactive phosphorus in nutrient-poor (oligotrophic) waters [1,8]. Some of these methods are sensitive to high chloride concentrations due to a phenomenon known as salt error [11]. In contrast, procedures involving ion association complexes (IAs) can be performed in highly saline solutions.

An alternative method to increase the sensitivity of the spectrophotometric determination of phosphate is based on the formation IA between HPA and cationic dyes such as triphenylmethane, rhodamine, or polymethine dyes (PDs) [5,6,8,14–16]. IA-based methods are superior to heteropolyblue-based methods in several important respects, including about an order of magnitude higher sensitivity, rapidity, less dependence on the conditions of analysis (nature of the reducing agent, time, degree of reduction, and acidity of the solution), and higher selectivity toward chloride ions or transition metals.

Typically, the formation of IA results in the spectra of the dye and the IA being identical or only slightly different. In this respect, one of the main problems with approaches using IAs is how to remove excess dye. Previously, extraction and sorption on a suitable filter followed by dissolution in an organic solvent have been proposed to separate excess dye [17,18]. The use of organic solvents does not allow these methods to be classified as "green" methods of analytical chemistry. Additional stages complicate and lengthen the determination process. As a result, the achieved increase in sensitivity remains unattractive for most practical applications. In addition, partial co-extraction of the simple dye salt as well as impaired reproducibility limit the sensitivity. Some of these drawbacks can be eliminated or minimized using microextraction separation of unreacted dye [19].

One of the best existing methods for the determination of phosphate using IA is based on the conversion of the weakly colored protonated dicationic form of malachite green (MG) into an intensely colored single-charged form. The latter arises as a result of the formation of the IA of 12-MPA with the dye due to a shift in acid–base equilibrium [5,20–22]. The MG method is 3–4 times more sensitive than the molybdenum blue method and does not require a separation step. However, the formation of IA between triphenylmethane dye and HPA is slow, and the absorbance of the colored product can rise for many hours, especially in samples with low orthophosphate concentration [21]. Because of the use of micellar medium for IA solubilization and high acidity, not more than one or two MG cations are usually attached to 12-MPA [4]. Furthermore, because relatively high concentrations of molybdate and MG are used, a precipitate is formed in the mixed reagent solution, which must be filtered before the sample is analyzed. This requires preparation of the color reagent on the day of use and makes the method time-consuming [23].

Another extraction-less method utilizes changes in the dye spectra occurring during the formation of the IAs of HPAs with cationic dyes [16,24]. We have previously found that the reaction of sufficiently large and hydrophobic anions with cationic dyes is always accompanied by characteristic changes in the absorption spectra. This can be successfully used for the determination of the corresponding substances [25]. An important prerequisite for such reactions is a sufficiently low solubility of the resulting IA. It is worth noting that the same specific IAs are formed using the MG method.

Representatives of any cationic dyes, at least triphenylmethane, rhodamine, and polymethine dyes, as well as anionic dyes [26], can enter into reactions of such type. The reaction is very fast, simple, and direct. However, the sensitivity achieved was high but not maximum. Considering the molar absorptivities of the PDs reaching

$3 \times 10^5$ L $mol^{-1}$ $cm^{-1}$ [27] and the attachment of 3–6 PD cations to HPA, the molar absorptivity of IA and sensitivity of the method can be greatly improved. The working wavelength is usually chosen at the positive maximum of the difference spectrum of IA and dye. At this wavelength, the IA absorbs light significantly less than at the maximum of the dye spectrum. Some variants of this method use surfactants to prevent precipitation of IA [28], which can be a major source of sample contamination. Nevertheless, the use of surfactants is not mandatory. At IA concentrations less than 1 μM, the supersaturated phase of IA in solution is stable, and the absorbance remains unchanged for at least several hours.

The formation of IA nanoparticles can be used to develop other approaches. They are based on dye luminescence quenching and strong resonance scattering of incident light on IA nanoparticles [15,29–31]. The measurement of scattered light is poorly reproducible, especially at low concentrations, and the estimation of the small difference in fluorescence intensity required at the lower end of analyte concentrations is also subject to large fluctuations. These reasons reduce the attractiveness of these methods.

Automation of reactions using IAs faces difficulties associated with the sorption of sparingly soluble IA precipitate on the tube walls of the flow system. It has recently been shown that such difficulties can be minimized by using IA 12-heteropolymolybdates of phosphorus and silicon with the polymethine dye Astra Phloxine, provided that a sufficiently low concentration of the IA, less than 1 μM, is present in solution [16]. This allowed us to develop a highly sensitive and selective method for the consecutive determination of these elements.

In this work, a new approach to eliminate the influence of dye excess based on the selective oxidation of excess PD ions that are not part of IA is proposed for analytical methods using IA formation. The applicability of this approach was demonstrated by the development of a simple, highly sensitive, and selective method for the determination of orthophosphate as an IA of 11-molybdovanadophosphate HPA (11-MVP) with PD. Three representatives of PDs were studied, namely diindodicarbocyanine (DIDC), N,N′-dipropyldiindodicarbocyanine (Pr-DIDC), and diindotricarbocyanine (DITC). The chemical structure of the dyes is shown in Figure 1. Chemometric optimization based on full factorial experimental design was used to find the optimum conditions. The developed method was applied to the determination of phosphate in water samples.

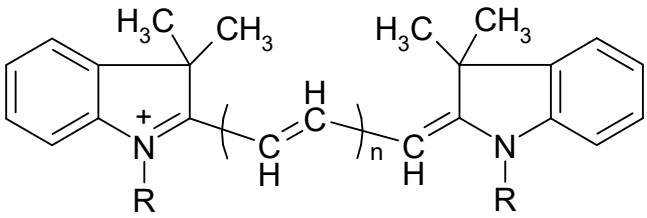



**Figure 1.** Chemical structure of polymethine dyes. DIDC—R = $CH_3$, $n$ = 2; Pr-DIDC—R = $C_3H_7$, $n$ = 2; DITC—R = $CH_3$, $n$ = 3.

## 2. Results and Discussion

### *2.1. Investigation of Oxidation of Polymethine Dyes in the Presence of Heteropolyanion and Oxidant*

In a preliminary study, it was established that symmetrical carbocyanine, dicarbocyanine, and tricarbocyanine dyes are capable of being oxidized under the action of sufficiently strong chemical oxidants. The reaction of such PDs with several oxidizing agents, namely potassium permanganate, potassium dichromate, cerium (IV) sulfate, potassium nitrate, potassium chlorate, potassium perchlorate, potassium iodate, potassium persulfate, potassium periodate, potassium bromate, sodium nitrite, and sodium vanadate, was investigated.

The reaction was carried out in the presence of phosphate and molybdate. The acidity was chosen to be optimal for the formation of HPA. Under these conditions, the formation of isopolyanions and further formation of IAs with PDs can be excluded. It was found that phosphate, molybdate, and 12-molybdophosphate do not oxidize PDs.

The rate of PD oxidation correlates with the strength of the oxidant (Figure 2). Potassium dichromate, sodium nitrite, and cerium (IV) sulfate require 2–3 min to oxidize DIDC, whereas the reaction with permanganate occurs almost instantaneously. For the first three oxidizing agents, partial destruction of the dye in IA was observed. Permanganate completely oxidizes the dye ions that are part of the IA. Other oxidants studied oxidize DIDC too slowly. The use of an acidified mixture of molybdate and vanadate as both reagent and oxidant allows selective oxidation of only free dye ions not bound by HPA. Therefore, this mixture was chosen as the oxidizing agent. It was taken into account that IA in this case had the highest molar absorptivity, and the reproducibility of the results obtained with this reagent was the best. Also, compared to 12-molybdophosphate, mixed 11-MVP was found to be more stable in the strongly acidic medium used in the oxidation reaction studied. Other PDs including Astra Phloxine were stable to oxidation by most oxidizing agents tested. The mixture of Fe (II) and $H_2O_2$ used previously for the oxidation of DIDC [32] was excluded from consideration because $H_2O_2$ can degrade HPA, given the well-known ability of molybdenym (VI) and vanadium (V) to form stable peroxo complexes.

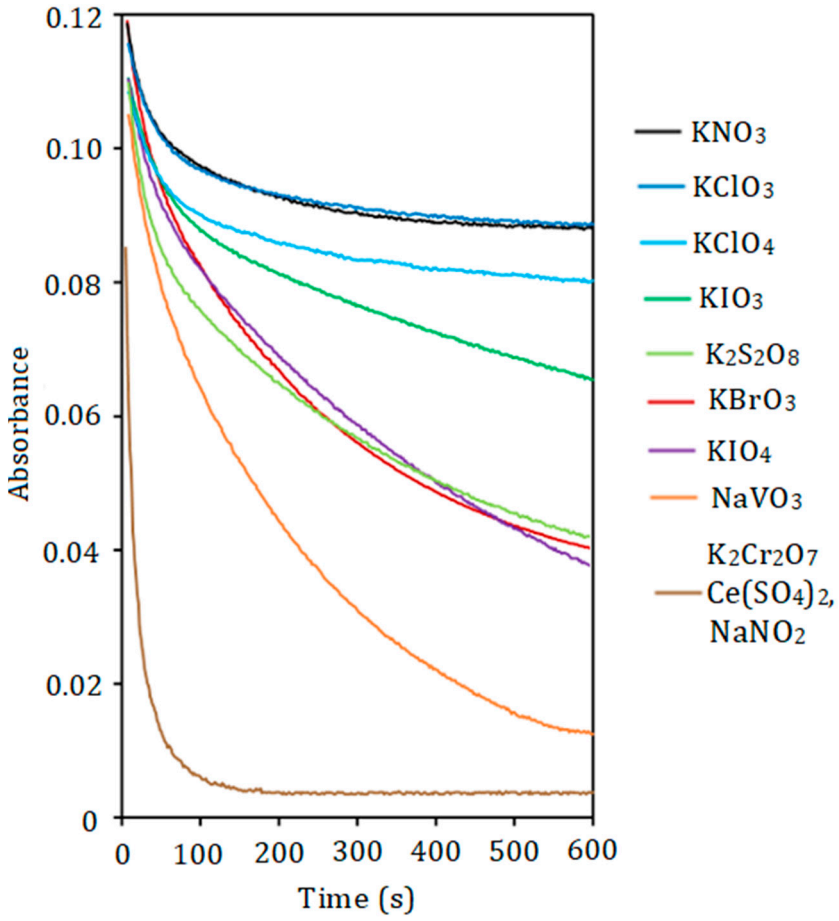



**Figure 2.** The effect of oxidant nature on the absorbance of DIDC. DIDC 1.0 μM, $KH_2PO_4$ 2.0 μM, $Na_2MoO_4$ 0.43 mM, oxidant 0.10 mM, $HNO_3$ 0.22 M, $\lambda$ = 636 nm, $l$ = 1 cm.

For all of the oxidants studied, the product of the reaction is yellow in color, indicating that the chromophore chain remains long enough. The curve of potentiometric titration of

DIDC with potassium dichromate or cerium (IV) sulfate (Figure 3) has an inflection point corresponding to the fact that the dye loses two electrons. The following reaction scheme based on hydroxylation by the oxidation of DIDC or Pr-DIDC is proposed:

$$\text{R-CH = CH-CH = CH-CH = R} + 2[\text{O}] - 2e \rightarrow \text{R-CHOH-CHOH-CH = CH-CH = R}$$

The oxidation of polyenes by various oxidants catalyzed by high-valent ($d^0$) transition metals (V (V), W (VI), and Mo (VI)) usually leads to the formation of epoxides under mild conditions and to diols in the presence of water [33]. Another oxidation scheme was proposed in [32] with the cleavage of the double bond in DIDC by using the Fenton reagent, which had a high oxidation potential of 2.0–2.8 V and is characterized by the generation of a hydroxyl radical. The data obtained in the electrochemical oxidation of PDs, in particular DIDC and DITC [34–36], allowed us to conclude that the radical dications formed during one-electron oxidation undergo irreversible dimerization at even-methine carbon atoms.

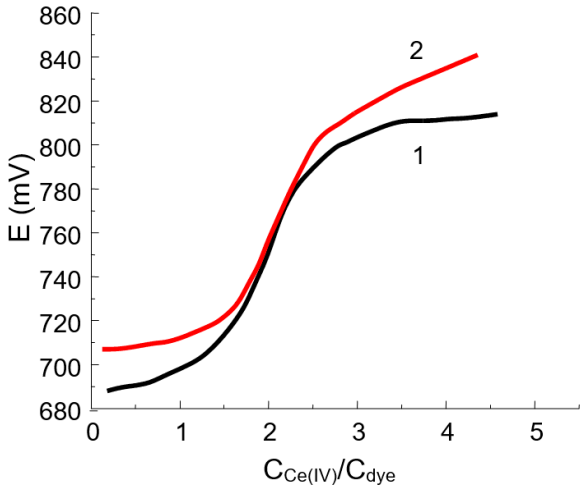



**Figure 3.** Titration curves for 10 mL of 0.112 mM DIDC (1) and 10 mL of 0.134 mM Pr-DIDC (2) with 1 mM cerium (IV) sulfate.

PDs are converted to the colorless form by protonation in a sufficiently acidic solution (Table 1). The range of existence of the cationic forms of DIDC and Pr-DIDC is wider than for DITC. While DIDC is stable up to 1 M acid, the protonation of DITC is considerable even at pH > 1, which makes it impossible the use of some oxidizing agents. At the same time, sufficiently high acidity is required for the formation of heteropolyanion, and the oxidizing power of the most commonly used reagents increases at low pH. The strength of the dyes used as reducing agents increases in the following order: DIDC ≅ Pr-DIDC < DITC. Only sufficiently strong oxidants having a standard oxidation-reduction potential of approximately 1.0 V or more are able to interact with DIDC or Pr-DIDC.

**Table 1.** Spectral, acid–base, and redox properties of DIDC, Pr-DIDC, and DITC as well as their IA with 11-MVP.

| Parameter | DIDC | Pr-DIDC | DITC |
|---|---|---|---|
| $\lambda_{max}^{dye}$ (nm) | 636 | 641 | 748 |
| $\varepsilon_{dye}$ ($mol^{-1}$ L $cm^{-1}$) | $1.82 \times 10^5$ | $1.75 \times 10^5$ | $2.32 \times 10^5$ [37] |
| $pK_p$ | −0.05 [38] | - | 1.03 [38] |
| $pK_h$ | 12.77 [39] | - | 11.84 [38] |
| $E^o$ (V) (vs. SHE) [1] | 0.918 | 0.933 | 0.700 |
| $E_{1/2}^{ox}$/(vs. $Fc^+$/Fc) [2] | 0.287 [35] | - | 0.066 [35] |
| $\lambda_{max}^{IA}$ (nm) | 600 | 630 | 640 |
| $\varepsilon_{IA}$ ($mol^{-1}$ L $cm^{-1}$) | $1.86 \times 10^5$ | $1.72 \times 10^5$ | $0.42 \times 10^5$ |

[1] Standard hydrogen electrode. [2] Ferrocene oxidation potential.

*2.2. Changes in Absorption Spectra During the Reaction Between PDs and Vanadate*

The IA spectrum differs significantly from the dye spectrum as a result of the reaction between HPA and DIDC (Figure 4) [16,24]. The solution spectra of the system under study represent the sum of the spectra of the oxidized and reduced forms of the dye, as well as the IA spectrum of DIDC with HPA. After 15–20 min, the oxidation of the excess dye is complete, and only IA remains in the reaction mixture. The spectrum of IA or actually aggregated dye consists of several strongly overlapping bands and has no pronounced maximum (Figures 4 and 5a). As can be seen particularly well from the difference spectrum (Figure 5c), the dye band at 636 nm completely disappears. Instead, two bands appear in the spectrum at approximately 540 and 680 nm, shifted hypso- and batochromically with respect to the main dye band (Figure 5c). It is worth noting that a completely similar IA spectrum can be obtained without oxidation under conditions of large excess of counterion. The DIDC spectrum obtained in a tenfold excess of 11-MVP (Figure 4) contains the same three bands that were observed in the IA spectrum remaining after oxidation of the dye excess.

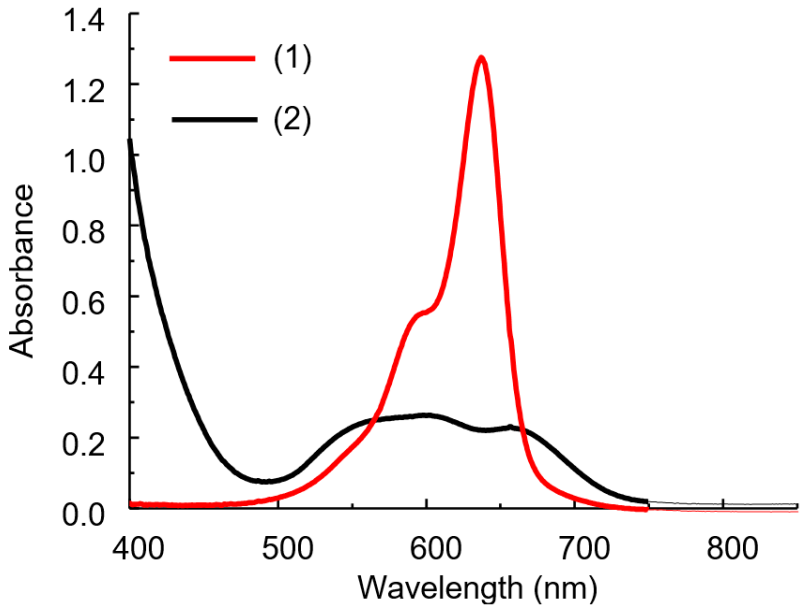



**Figure 4.** Absorption spectra of DIDC (1) and its IA with 11-MVP in the excess of HPA (2). DIDC 0.01 mM, $KH_2PO_4$ 0.1 mM, $Na_2MoO_4$ 0.43 mM, $NaVO_3$ 0.041 mM, $HNO_3$ 0.22 M, $l$ = 1 cm.

In the spectrum of the dye after oxidation, the band at 636 nm disappears, whereas two new bands appear at 400 and 490 nm (Figure 5b). Two bands with a similar position were observed in the spectrum of the PD obtained by electrochemical oxidation [34].

During the first ten minutes, a large negative difference is observed in the spectrum obtained by subtracting the spectrum of the blank solution from the IA spectrum (Figure 5c). The analytical signal corresponding to the dye maximum at 636 nm is high, but it cannot be measured with adequate reproducibility due to the very rapid oxidation of the dye. However, the absorbance measured at 600 nm becomes constant after 15–20 min, is easily reproducible, and is linearly related to the phosphate concentration. The isobestic point, present in all systems studied (Figure 5), indicates the interconversion of the reduced and oxidized forms of free dye ions. At the same time, the spectrum of the IA remains unaltered due to the rapid formation of this complex.

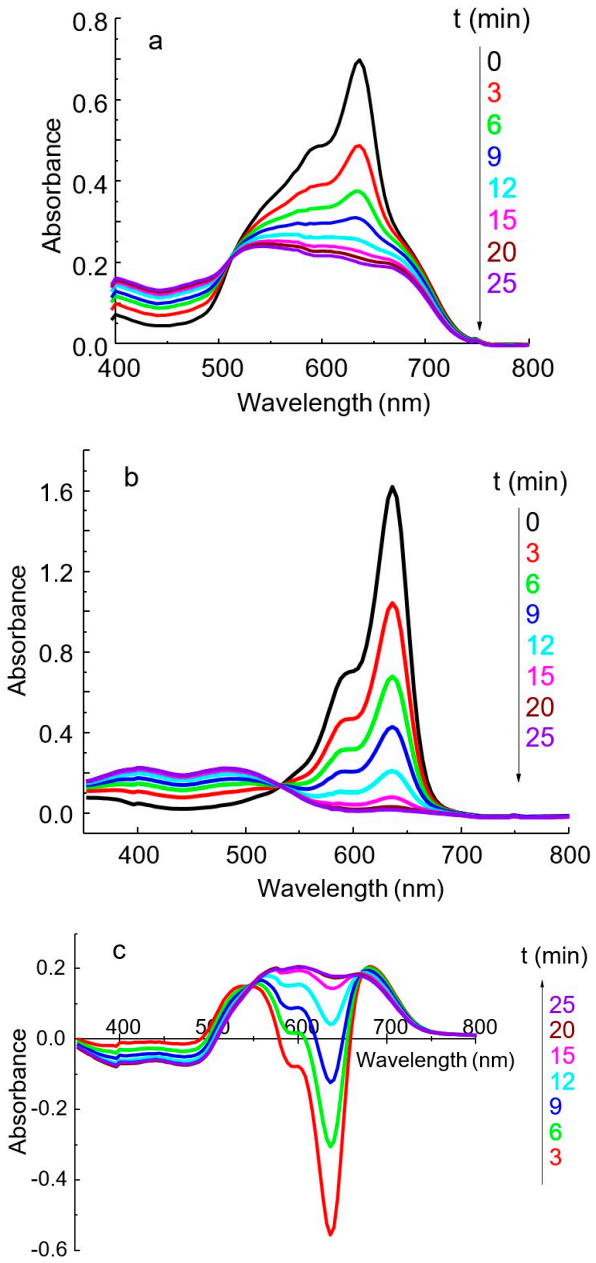



**Figure 5.** The effect of oxidation time on the absorption spectra of IA $PVMo_{11}O_{40}^{4-}$ DIDC (**a**), reagent blank (**b**), and the difference between a–b (**c**). DIDC 0.015 mM, $KH_2PO_4$ 2.0 μM, $Na_2MoO_4$ 0.43 mM, $NaVO_3$ 0.041 mM, $HNO_3$ 0.22 M, *l* = 1 cm.

### *2.3. The Theoretical Background of Studied Reactions*

The theory of self-aggregation of organic dyes can satisfactorily explain both the changes in the absorption spectra of PDs resulting from the formation of IA with 12-MPC and the selective oxidation of free dye ions. Self-aggregation of organic molecules has attracted interest in recent years in both fundamental and applied fields due to its novel chemical, physical, and optical properties. Self-aggregation of dyes in solution is a frequently occurring phenomenon in the chemistry of organic dyes due to the strong π–π dispersion interaction between the conjugated system of π-electrons in these molecules [27,40–44]. In the reactions studied in this work, conditions were created for forced convergence of dye cations as a result of the formation of sparsely soluble nanodispersed particles of IA. In this case, the π–π-dispersion interaction of the chromophoric–aromatic system of dyes increases, which, in accordance with the exciton theory, leads to the splitting of the excited electron level into two

levels with lower and higher energy. The transition of electrons to these levels results in the appearance of one or two hypso- and/or bathochromically shifted bands in the absorption spectrum relative to the main dye band.

Aggregation of dyes in aqueous solution can be promoted by a number of different factors, starting with the well-known self-association phenomenon that occurs with increasing dye concentration. Aggregation can be also enhanced by sorption of the dye on the surface of crystals such as AgCl [45] or by binding to neighboring charged sites on polyelectrolyte molecules [46]. High concentrations of inorganic salts can have a significant effect on the formation of PD aggregates, which is explained by the decreased solubility of the formed IAs in concentrated salt solutions [47,48].

We have previously shown that a stable supersaturated solution of IA can be formed during the reaction between PD and HPA [16] or other large anions such as $BiI_4^-$ [25] due to the very low solubility of such IAs. The close contact between the molecules of IA in poorly soluble precipitate particles favors the noncovalent interaction of the PD cations with each other.

To explain the difference in the oxidation rate between free dye ions and those bound into IA, it can be assumed that the dye ions in IA are more or less isolated from contact with the oxidant in these aggregates, which strongly slows down their rate of oxidation. However, another hypothesis seems more reasonable. It is well known that aggregation can cause a change in the formal redox potential for the dye. The oxidation potential of the one-electron transition for the J-aggregate of 3,8:3,12-dimethylene-9,11-neopentylenethiadicarbocyanine-p-toluenesulfonate was 74 mV more positive compared to the similar value for the monomer [49]. In contrast to these data, the redox potential of the oligostreptocyanin dimer was shifted to the negative potential region by 0.22 V relative to the monomer from 0.98 V to 0.76 V [50]. In [51], the redox potential of thiacarbocyanine PD was shown to be shifted to the negative potential region from 0.96 V for the monomer to 0.78 V for the J-aggregate.

Thus, depending on the nature of the dye and the environment, different directionality of the oxidation potential during aggregation can be observed. In our case, aggregation leads to an increase in the oxidation potential of the dye contained in IA. Consequently, free dye ions, which have a more negative redox potential, react more easily with oxidizing agents. These data explain the stability of PD ions in the composition of IA with HPA by weakening of their reducing properties due to the formation of aggregates.

As has been shown in a number of articles [49,52], the oxidation potentials of PDs strongly decrease with increasing length of the polymethine chain. The data we obtained confirm this observation (Table 1). When selecting the optimal oxidant for the reaction under study, the highest selectivity for oxidation of only unbound dye ions will be observed if the redox potential of the oxidant used is between the redox potentials for free and IA-bound dye. Presumably, this range is between 0.7 (IA-bound dye) and 0.9 V (free dye). The standard redox potentials for the studied oxidants increase in the series 1.004 V ($VO_2^+/VO^{2+}$) < 1.232 V ($Cr_2O_7^{2-}/2Cr^{3+}$) < 1.44 V ($Ce^{4+}/Ce^{3+}$) < 1.51 V ($MnO_4^-/Mn^{2+}$). As can be seen from this series, the best agreement with the put forward assumption is observed for the vanadate system, which also explains the observed difference in the rate and completeness of dye oxidation in IA particles and in solution.

### *2.4. Optimization of the Conditions for the Determination of Orthophosphate*

The optimal conditions for the formation of 11-MVP are well known [53]. In all experiments, the molar ratio of Mo to V was fixed at 11:1, and the concentrations of molybdate and vanadate were taken as 0.43 mM and 0.041 mM, respectively.

The oxidation of PDs with vanadate is a slow reaction. The measured absorbance is highly dependent on the reaction time, the acidity used, and the dye concentration. The effect

of these factors on the oxidation of DIDC, Pr-DIDC, and DITC by vanadate was studied using two-factor optimization and a response surface study. Optimal conditions for phosphate determination can be selected by studying the response surface since the three-dimensional picture gives a complete overview of the system. Because the number of significant factors in the studied system was more than two, one of the factors should be excluded to visualize the response surface. At the 95% confidence level ($p < 0.05$), weaker significance was observed for the dye concentration variable. Therefore, this factor was set at 0.015 mM as a compromise between the maximum response and acceptable absorbance of the blank solution. The effect of reaction time and acidity on IA absorbance is presented in Figure 6a.

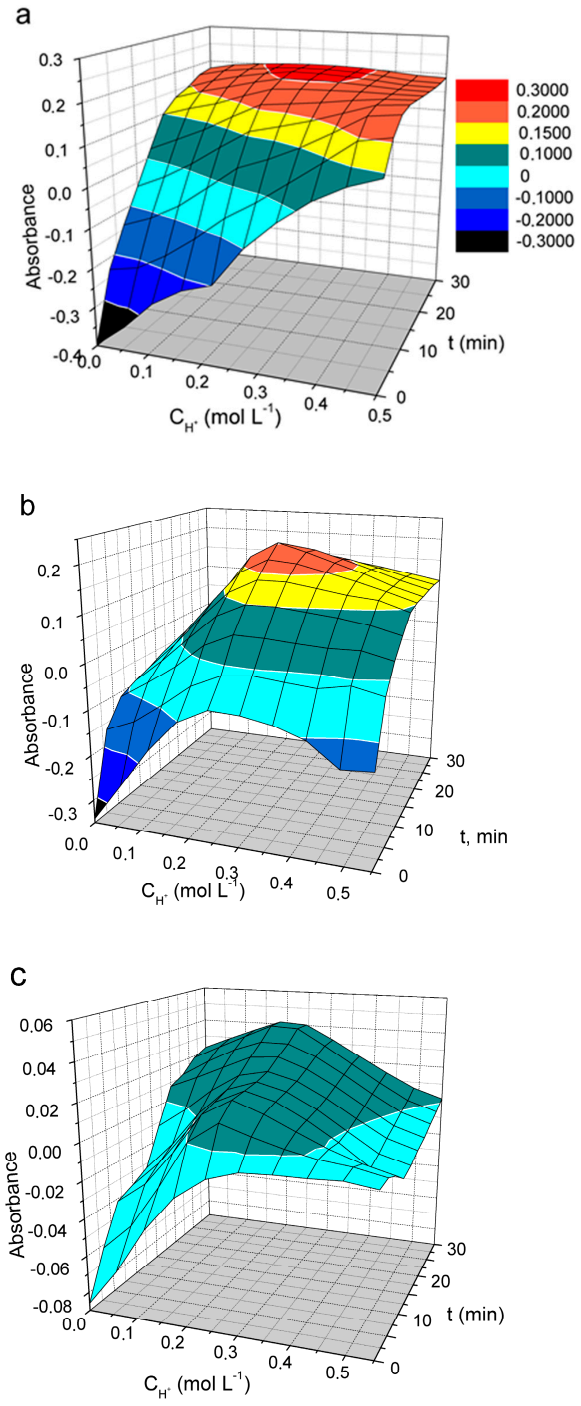



**Figure 6.** The effect of acid concentration and time of oxidation on the absorbance of IA DIDC-MVP (**a**), Pr-DIDC-MVP (**b**), and (**c**) DITC-MVP. Conditions: 0.43 mM $Na_2MoO_4$, 0.041 mM $NaVO_3$, 2 µM $KH_2PO_4$, 0.015 M PD, $l$ = 1 cm, $\lambda$ = 600 nm (DIDC); $\lambda$ = 630 nm (Pr-DIDC); $\lambda$ = 640 nm (DITC).

The most suitable results were obtained by using DIDC because it was the only dye for which the absorbance remained constant over the wide range of variables studied. Only a maximum instead of a plateau was observed on the response surface for Pr-DIDC (Figure 6b). During storage, DITC is oxidized by oxygen dissolved in water. Therefore, it was not surprising that in this case, even the dye included in the IA was oxidized by the oxidant used, leading to strong variations and low values in the absorbance (Figure 6c). DIDC was selected to further optimize the optimal conditions for the determination of phosphate.

At the same time, the influence of the third factor on absorbance, namely the concentration of the dye, is significant. Thus, all three factors were found to be interdependent. In this case, a common option for finding optimal conditions is optimization by developing an empirical model of the response surface by the full factorial design.

### *2.5. Search of the Optimal Conditions by the Full Factorial Design*

Optimization procedures are usually based on univariate optimization, which facilitates the interpretation of the results obtained but does not take into consideration the interactions between variables. Consequently, a false maximum may be attained, leading to the use of certain conditions under which the combination of variables does not provide the best analytical response. One commonly used approach of multivariate tools is the two-level full factorial design. However, preliminary calculations using this empirical model, as well as inspection of experimental response surfaces (Figure 6), show that second-order effects on the response must be accounted for.

The number of trials to be conducted in the 33 factorial design was reduced by using a central composite design. It consisted of a $2^k$ (k = 3, number of factors) factorial design, which provided data for estimating the first-order effects for each factor and the interactions between the factors and a "star" design consisting of 2k + 1 points that provided data to estimate second-order effects. Three factors, (1) dye concentration, (2) acid concentration, and (3) reaction time, could be systematically varied and optimized in the studied system (Table S1). A detailed description of chemometric optimization by full factorial design can be found in Supplementary Material.

The effects of individual factors and their combinations were determined (Table S2). According to these studies, all three effects studied are significant, with acid concentration having the greatest influence. The interactions (acid concentration × dye concentration) and (acid concentration × time) are also statistically significant. In the Pareto chart (Figure 7), positive values represented by time and acid concentration indicate that upon their increase, the response also increases, while a negative value for dye concentration means that this factor has the opposite effect (Table S3).

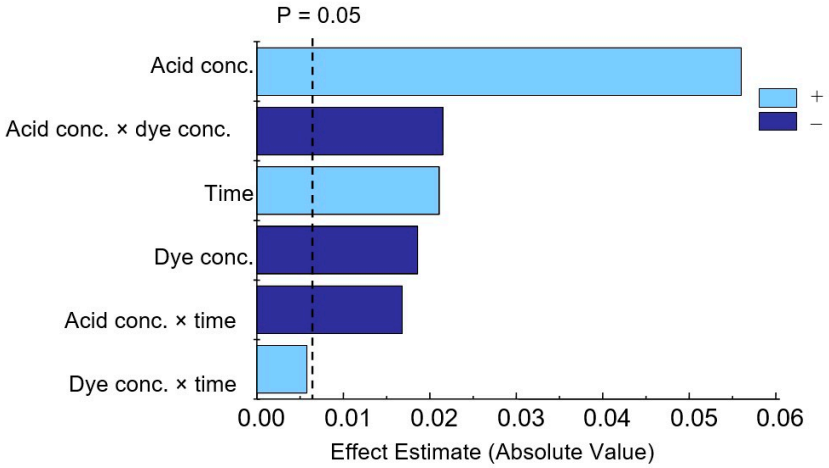



**Figure 7.** Pareto chart of standardized effects for variables in phosphate determination.

In summary, the optimal conditions for spectrophotometric determination of phosphate with IA DIDC-MVP are 0.3 M nitric acid, 0.015 mM DIDC, and 18 min of reaction time. These values agree well with two-factor optimization results and the experimentally obtained response surface (Figure S1).

## 3. Analytical Performance

### *3.1. Method Validation*

Based on the found optimal conditions, a spectrophotometric procedure for the determination of orthophosphate was developed. Its analytical characteristics are summarized in Table 2. The limit of detection (LOD) and limit of quantification (LOQ) were calculated according to the equations LOD = 3 × $S_a$/b and LOQ = 10 × $S_a$/b, where $S_a$ is the standard deviation of the regression. The molar absorptivity of IA DIDC-MVP obtained from the slope was equal to 1.85 × $10^5$ $mol^{-1}$ L $cm^{-1}$.

**Table 2.** Characteristics of the proposed procedure and calibration curve.

| Characteristics | Value |
|---|---|
| λ (nm) | 600 |
| Reaction time (min) | 18 |
| Path length (cm) | 5 |
| Calibration range (μM) | 0.04–0.4 |
| Correlation coefficient | 0.9991 |
| Intercept ± Δ | 0.246 ± 0.012 |
| Slope ± Δ | (9.3 ± 0.5) × $10^5$ |
| LOD (μM) | 0.013 |
| LOQ (μM) | 0.04 |
| Molar absorptivity ($mol^{-1}$ L $cm^{-1}$) | 1.86 × $10^5$ |

### *3.2. Evaluation of Interference*

The effects of potential interferences from ions that commonly accompany phosphorus (V) in natural and wastewater were investigated by the determination of 0.4 μM orthophosphate according to the recommended procedure. These species were largely tolerated without any pre-treatment. An ion was considered not to interfere if a relative error caused by it was less than 5%. The maximum tolerable concentrations of 23 foreign ions are given in Table 3 and, in general, significantly exceed the reported concentration levels of common pollutants in natural waters [12]. This indicates the high selectivity of the proposed method. However, $AsO_4^{3-}$, $Fe^{3+}$, and $WO_4^{2-}$ ions introduce serious interferences to phosphate at molar ratios of 20:1 and 15:1, respectively. Silicate affects the determination of phosphate starting from 0.2 mM.

**Table 3.** Tolerance levels of foreign ions in the determination of 0.4 μM orthophosphate.

| Foreign Species | Tolerance Level (mM) |
|---|---|
| $SO_4^{2-}$ | 225 |
| $Cl^-$, $NH_4^+$ | 100 |
| $Na^+$, $Li^+$, $K^+$, $Ca^{2+}$, $Br^-$ | 50 |
| $Mn^{2+}$, $Mg^{2+}$ | 20 |
| $Ni^{2+}$ | 6 |
| $Zn^{2+}$ | 5 |
| $Co^{2+}$, $Cu^{2+}$, $CO_3^{2-}$ | 2 |
| $I^-$ | 1 |
| $CH_3COO^-$ | 0.4 |
| $SiO_3^{2-}$ | 0.2 |
| $Pb^{2+}$ | 0.2 |
| $F^-$ | 0.08 |
| $AsO_4^{3-}$ | 0.01 |
| $Fe^{3+}$ | 0.01 |
| $WO_4^{2-}$ | 0.006 |

### 3.3. Analytical Application

The developed method was applied to the determination of phosphate in deep-well waters. The results obtained by the proposed method, the method using the formation of IA between Astra Phloxine and 12-molybdophosphate, and the standard method are presented in Table 4. The confidence intervals of the results of water analysis obtained by all three methods overlap each other, which confirms the accuracy of the developed method.

**Table 4.** Determination of phosphate in deep-well water.

| Sample | Proposed Method | | IA 12-Molybdophosphate-Astra Phloxine FF [24] | | Molybdophosphate Blue [12] | |
|---|---|---|---|---|---|---|
| | (C ± Δ) [1] (μM) | RSD [2] (%) | (C ± Δ) (μM) | RSD (%) | (C ± Δ) (μM) | RSD (%) |
| Artesian water | 6.1 ± 0.3 | 4 | 6.3 ± 0.3 | 4 | 6.3 ± 0.4 | 5 |
| Mineral water "Morshinska" | 1.11 ± 0.06 | 4 | 1.23 ± 0.08 | 5 | 1.07 ± 0.08 | 6 |
| Mineral water "BonAqua" | 0.42 ± 0.03 | 5 | 0.41 ± 0.02 | 4 | <LOQ | - |

[1] Δ—confidence limit ($n$ = 5, $p$ = 0.95). [2] RSD—relative standard deviation.

### 3.4. Comparison of the Present Method with Previous Methods for Orthophosphate Determination

A comparison of the different methods developed for the determination of orthophosphate from 2019 to the present is presented in Table 5. Spectrophotometric methods based on the reduction of12-MPA by ascorbic acid and the formation of heteropolyblue remain in the spotlight. They are often combined with modern preconcentration methods and automated with flow methods of analysis. IAs are also used as analytical forms in combination with three detection methods, namely UV–Vis spectrophotometry, resonance Rayleigh scattering, and fluorescence. In terms of sensitivity, the method developed in this work competes confidently with all recently proposed methods. The advantage over methods based on the formation of heteropolyblue is due to the much higher molar absorption coefficient of IA DIDC-12-MPA, almost an order of magnitude higher. For heteropolyblue, it ranges from 15,000 to 24,000 $mol^{-1}$ L $cm^{-1}$ depending on the method. For the same reason, the sensitivity of the present method is superior or equal to methods using UV–Vis detection and preconcentration. The absolute limit of detection of most electrochemical, chromatographic, and atomic spectroscopic methods is also lower than that of the proposed method, although it should be noted that this table does not include methods developed before 2019. The greenness of the developed method was evaluated using the Analytical Greenness (AGREE) metric (Figure 8). The obtained score of 0.62 confirms its sufficiently high environmental friendliness.

**Table 5.** Comparison of methods proposed for the determination of orthophosphate in 2019–2025.

| Method | Description of the Method | LOD (μg $L^{-1}$) | Linear Range (μg $L^{-1}$) | Ref. |
|---|---|---|---|---|
| Molecular spectroscopy methods | | | | |
| UV–Vis | Formation of molybdenum blue by reduction in 12-MPA using bismuth (III) and antimony (III) as sensitizers | 13 | 20–1800 | [54] |
| UV–Vis | Formation of IA between malachite green and 12-MPA | 7 | Up to 300 | [23] |
| RRS | Formation of IA between cationic methyl violet and 12-MPA | 4 | 8–200 | [15] |
| Chemical sensor | Portable pump/valve-free water quality sensor based on phosphomolybdenum blue method | 12 | - | [55] |
| PTLS | Formation of molybdenum blue by reduction in 12-MPA | 4 | 11–1000 | [56] |
| UV–Vis, RRS, FL | Formation of IA between Nile blue and 12-MPA | 4.8, 4.9, 5.2 | 5–100 | [57] |
| Flow methods of analysis | | | | |
| SIA-UV–Vis | The molybdenum blue method using antimony and ascorbic acid | 7.7 | Up to 2000 | [58] |
| Microfluidic SIA | A miniaturized microfluidic hydrodynamic sequential injection system based on molybdenum blue method | 1.5 | 3–30 | [59] |

**Table 5.** *Cont.*

| Method | Description of the Method | LOD (μg $L^{-1}$) | Linear Range (μg $L^{-1}$) | Ref. |
|---|---|---|---|---|
| μPAD | Phosphomolybdenum blue method with antimony (III) as catalysator and ascorbic acid as reducing agent | 1.5 | 5–100 | [60] |
| FB-SP analyzer | Formation of molybdenum blue by reduction of 12-MPA | 4 | Up to 360 | [61] |
| Combination of UV–Vis spectrophotometry with preconcentration method | | | | |
| MEPS-UV–Vis | Extraction of molybdoantimonatophosphoric heteropoly blue with hydrophobic C18 sorbent packed into a MEPS, elution with 60 μL of acetonitrile | 0.4 | 1.3–24.8 | [62] |
| Indirect UV–Vis | Separation of 12-MPA by extraction with isoamyl acetate, re-extraction with into aqueous phase, and formation of complex between molybdenum (VI) and sulfonitrazo | 10 | 20–430 | [63] |
| CPE-UV–Vis | Room temperature CPE with Triton X-100 procedure based on the heteropoly blue formation | - | 1.6–63 | [64] |
| MME-UV–Vis | Extraction of heteropoly blue with supramolecular solvent (alkyl polyglucoside and carboxylic acid) | 5 | 20–400 | [65] |
| Electrochemical methods | | | | |
| CV | CV via $[Omim]_6Mo_7O_{24}$—carbon paste electrode | 2.6 | 3–3 × $10^5$ | [66] |
| APSE | Phosphate-selective electrode with a plasticized membrane that includes bis(2-ethylhexyl)tin (IV) dichloride as an ionophore | 24 | 60–3000 | [67] |
| Chromatography | | | | |
| CZE | Determination of phosphate in seafood by CZE with indirect UV–Vis detection | 1.1 mg $kg^{-1}$ | 5–55 mg $L^{-1}$ | [68] |
| IC | Suppressed IC after perchloric acid deproteinization in milk | 33 | 1000–60,000 | [69] |
| Atomic spectrometry methods | | | | |
| EDXRF | Ultrasonically assisted dispersive micro-solid phase extraction using lanthanum oxide supported on graphene oxide | 0.4 | 2–300 | [70] |
| LIBS | Laser-induced breakdown spectroscopy | 100 | - | [71] |
| UV–Vis | Formation of IA between DIDC and 11-MVP, oxidation of dye excess with vanadate | 0.4 | 1.2–12 | This study |

UV–Vis—Ultraviolet–Visible spectrophotometry; RRS—resonance Rayleigh scattering; PTLS—photothermal lens spectrophotometry; FL—fluorescence; SIA—sequential injection analysis; μPAD—microfluidic paper-based sensor; FB-SP analyzer—flow-batch syringe-pump-based flow analyzer; MEPS—microextraction by packed sorbent; CPE—cloud point extraction; MME—micellar microextractio; CV—Cyclic voltammetry; APSE—amperometric phosphate-selective electrode; CZE—capillary zone electrophoresis; IC—ion chromatography; EDXRF—energy dispersive X-ray fluorescence spectrometry.

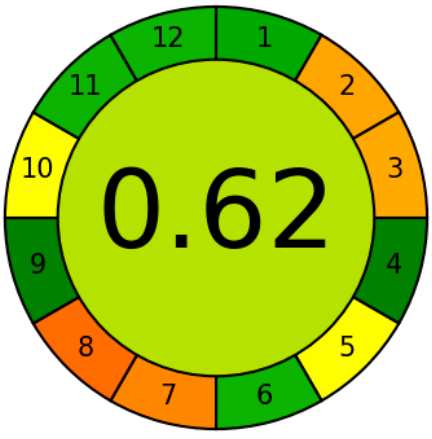



**Figure 8.** Assessment of the greenness of the proposed method by AGREE metric.

## 4. Materials and Methods

### *4.1. Reagents and Apparatus*

All chemicals used were of analytical-grade quality. Double distilled water was used throughout this experiment. A stock solution of phosphorus (V) containing 0.1 M phosphate was prepared by dissolving $KH_2PO_4$ in water. A 0.1 M molybdate solution was prepared by dissolving $Na_2MoO_4 \times 2H_2O$ recrystallized from water–ethanol mixture, standardized

by evaporation, weighed, and stored in a polyethylene bottle. DIDC iodide was purchased from Sigma-Aldrich, and the Pr-DIDC iodide and DITC fluoroborate were obtained as a gift from Prof. A.A. Ishchenko (Institute of Organic Chemistry, Kyiv, Ukraine).

A UV 4 UV–Vis spectrophotometer (Unicam, Great Britain) controlled by Software Vision 32-bit Version 1.10 was used to measure the absorption spectra. Glass cuvettes with path lengths of 1 and 5 cm were used.

Minitab Statistical Software 16.2.2. was used to perform statistical design of experiments.

### *4.2. Preparation of the Combined Reagent Solution*

A sample of $NaVO_3 \times 2H_2O$ weighing 0.065 g was dissolved in 5 mL of hot water; after cooling, 12.5 mL of concentrated $HNO_3$ was added, then 1.05 g of $Na_2MoO_4 \times 2H_2O$, and the solution was filled with distilled water to 100 mL. This solution was diluted five times before analysis. The final solution contained 8.6 mM molybdate, 0.3 M nitric acid, and 0.82 mM vanadate.

### *4.3. Procedure for Orthophosphate Determination*

A sample containing from 0.03 to 0.3 μg of orthophosphate was placed in a 25 mL volumetric flask. Then, 0.5 mL of the combined reagent solution, 1.5 mL of 2 M $HNO_3$, and 0.75 mL of 0.2 mM DIDC were added, and the solution was diluted to 10 mL. Absorbance was measured at 600 nm after 18–20 min against the reagent blank using a 5 cm cuvette.

### *4.4. Analysis of Water Samples*

Water samples were filtered through a 0.45 mm membrane filter to remove particulate matter and immediately analyzed. Next, the procedure for the determination of phosphate in real samples was performed as described in the calibration. At least five repeated measurements were taken for each sample.

## 5. Conclusions

A new approach has been proposed to eliminate the influence of dye excess in reactions that utilize the formation of an ion-association complex between a heteropolyanion and an organic dye. It is based on the selective oxidation of a polymethine dye with a suitable oxidizing agent. It is shown that symmetric diindodicarbocyanine and diindotricarbocyanine PDs can be oxidized by sufficiently strong oxidants. The selective decolorization of only free dye ions as well as the strong changes in the IA spectrum compared to the dye spectrum can be explained by the isolation of the dye in the sparingly soluble IA nanoparticles and the change in the formal redox potential of the aggregated dye. A mixture of vanadate and nitric acid was chosen as the oxidizing agent. Although this reaction is slower than the reaction with potassium dichromate or cerium (IV) sulfate, it is more reproducible and has a lower limit of detection. Of the three dyes investigated, including DIDC, Pr-DIDC, and DITC, the best results were obtained with DIDC. The presented method describes a new route towards an eco-friendly methodology that eliminates the use of organic solvents in ionic associate-based assay procedures. The developed method is simple, highly sensitive, and selective. Its applicability was successfully tested for the determination of phosphate in several types of natural waters.

**Supplementary Materials:** The following supporting information can be downloaded at: https://www.mdpi.com/article/10.3390/molecules30091872/s1, Figure S1: Response surface for IA absorbance as a function of acid concentration and reaction time at a constant dye concentration of 0.015 mM; Description of multivariate optimization of conditions for the determination of orthophosphate using the formation of IA between 11-molybdovanadophosphate HPA with DIDC and oxidation of excess dye; Table S1: Factors and their levels for a factorial experiment; Table S2: Design

matrix and response values in the 33 central composite factorial design; Table S3: Estimation of model parameters for constructing a response surface.

**Author Contributions:** Conceptualization, A.B.V. and Y.B.; data curation, A.B.V.; formal analysis, S.V.K. and I.E.B.; funding acquisition, Y.B.; investigation, A.B.V. and S.V.K.; methodology, A.B.V., Y.B., I.B. and I.E.B.; project administration, Y.B.; resources, Y.B. and I.B.; supervision, Y.B.; validation, A.B.V.; visualization, A.B.V. and I.E.B.; writing—original draft, A.B.V., S.V.K. and I.E.B.; writing—review and editing, A.B.V. and Y.B. All authors have read and agreed to the published version of the manuscript.

**Funding:** Funded by the EU NextGenerationEU through the Recovery and Resilience Plan for Slovakia under the project No. 09I03-03-V01-00106 (Andriy Vyshnikin). Funded by the Scientific Grant Agency VEGA of the Ministry of Education, Research, Development, and Youth of the Slovak Republic and the Slovak Academy of Sciences for their support (Grant no. 1/0177/23) (Yaroslav Bazel' and Andriy Vishnikin).

**Institutional Review Board Statement:** Not applicable.

**Informed Consent Statement:** Not applicable.

**Data Availability Statement:** The original contributions presented in the study are included in the article/Supplementary Materials, further inquiries can be directed to the corresponding authors.

**Conflicts of Interest:** The authors declare that they have no known competing financial interests or personal relationships that could have appeared to influence the work reported in this paper.

## References

1. Patey, M.D.; Rijkenberg, M.J.A.; Statham, P.J.; Stinchombe, M.C.; Achterberg, E.P.; Mowlem, M. Determination of nitrate and phosphate in seawater at nanomolar concentrations. *TrAC Trends Anal. Chem.* **2008**, *27*, 169–182. [CrossRef]
2. Worsfold, P.J.; Gimbert, L.J.; Mankasingh, U.; Omaka, O.N.; Hanrahan, G.; Gardolinski, P.C.F.C.; Haygarth, P.M.; Turner, B.L.; Keith-Roach, M.J.; McKelvie, I.D. Sampling, sample treatment and quality assurance issues for the determination of phosphorus species in natural waters and soils. *Talanta* **2005**, *66*, 273–293. [CrossRef] [PubMed]
3. Worsfold, P.J.; Monbet, P.; Tappin, A.D.; Fitzsimons, D.A.; McKelvie, I.D. Characterisation and quantification of organic phosphorus and organic nitrogen components in aquatic systems: A review. *Anal. Chim. Acta* **2008**, *624*, 37–58. [CrossRef]
4. Smith, V.H. Eutrophication of freshwater and coastal marine ecosystems a global problem. *Environ. Sci. Pollut. Res.* **2003**, *10*, 126–139. [CrossRef]
5. Motomizu, S.; Li, Z.-H. Trace and ultratrace analysis methods for the determination of phosphorus by flow-injection techniques. *Talanta* **2005**, *66*, 332–340. [CrossRef] [PubMed]
6. Estela, J.M.; Cerda, V. Flow analysis techniques for phosphorus: An overview. *Talanta* **2005**, *66*, 307–331. [CrossRef]
7. Dubovik, D.B.; Tikhomirova, T.I.; Ivanov, A.V.; Nesterenko, P.N.; Shpigun, O.A. Determination of silicon, phosphorous, arsenic, and germanium as heteropoly acids. *J. Anal. Chem.* **2003**, *58*, 802–819. [CrossRef]
8. Worsfold, P.; McKelvie, I.; Monbet, P. Determination of phosphorus in natural waters: A historical review. *Anal. Chim. Acta* **2016**, *918*, 8–20. [CrossRef]
9. Zhu, X.; Ma, J. Recent advances in the determination of phosphate in environmental water samples: Insights from practical perspectives. *TrAC Trends Anal. Chem.* **2020**, *127*, 115908. [CrossRef]
10. Zhu, Y.; Fang, T.; Ji, D.; Li, H.; Chen, J.; Ma, J. Recent advances and prospects in on-site spectrophotometric nutrient measurement in aquatic ecosystems. *TrAC Trends Anal. Chem.* **2024**, *175*, 117723. [CrossRef]
11. Nagul, E.; Mckelvie, I.D.; Wordsold, P.; Kolev, S.D. The molybdenum blue reaction for the determination of orthophosphate revisited: Opening the black box. *Anal. Chim. Acta* **2015**, *890*, 60–82. [CrossRef]
12. Clesceri, L.S.; Greenberg, A.E.; Eaton, A.D. (Eds.) *Standard Methods for the Examination of Water and Wastewater*, 20th ed.; American Public Health Association: Washington, DC, USA, 1998.
13. Mogashane, T.M.; Mapazi, O.; Motlatle, M.A.; Mokoena, L.; Tshilongo, J. A review of recent developments in analytical methods for determination of phosphorus from environmental samples. *Molecules* **2025**, *30*, 1001. [CrossRef] [PubMed]
14. Li, Z.; Oshima, M.; Sabarudin, A.; Motomizu, S. Trace and ultratrace analysis of purified water samples and hydrogen peroxide solutions for phosphorus by flow-injection method. *Anal. Sci.* **2005**, *21*, 263–268. [CrossRef]
15. Li, L.; Zhang, J.; Deng, Z.; Su, Z.; Bai, Y.; He, J. Determination of phosphate in food based on molybdenum yellow derivatization coupled with resonance Rayleigh scattering method. *Anal. Sci.* **2024**, *40*, 461–469. [CrossRef] [PubMed]

16. Vishnikin, A.; Hedjazi, M.; Al-Shwaiyat, M.; Skok, A.; Bazel, Y. Consecutive spectrophotometric determination of phosphate and silicate in a sequential injection lab-at-valve flow system. *Anal. Chim. Acta* **2023**, *1273*, 341464. [CrossRef] [PubMed]
17. Motomizu, S.; Wakimoto, Y.; Tôei, K. Solvent extraction-spectrophotometric determination of phosphate with molybdate and malachite green in river water and sea-water. *Talanta* **1984**, *31*, 235–240. [CrossRef]
18. Susanto, J.P.; Oshima, M.; Motomizu, S.; Mikasa, H.; Hori, Y. Determination of micro amounts of phosphorus with Malachite Green using a filtration–dissolution preconcentration method and flow injection–spectrophotometric detection. *Analyst* **1995**, *120*, 187–191. [CrossRef]
19. Pena-Pereira, F.; Cabaleiro, N.; de la Calle, I.; Costas, M.; Gil, S.; Lavilla, I.; Bendicho, C. Directly suspended droplet microextraction in combination with microvolume UV–vis spectrophotometry for determination of phosphate. *Talanta* **2011**, *85*, 1100–1104. [CrossRef]
20. Munõz, A.; Mas-Torres, F.; Estela, J.M.; Cerda, V. Evaluation of spectrophotometric methods for determination of orthophosphates by sequential injection analysis. *Anal. Chim. Acta* **1997**, *350*, 21–29. [CrossRef]
21. Baykov, A.A.; Evtushenko, O.A.; Avaeva, S.M. A malachite green procedure for orthophosphate determination and its use in alkaline phosphatase-based enzyme immunoassay. *Anal. Biochem.* **1988**, *171*, 266–270. [CrossRef]
22. Jin, Y. Validation of assay for measuring acetyl-coenzyme a carboxylase activity in grasses using malachite green. *Anal. Biochem.* **2025**, *697*, 115723. [CrossRef]
23. Gache, S.A.M.; Angelini, A.A.R.; Sabeckis, M.L.; Flecha, F.L.G. Improving the stability of the malachite green method for the determination of phosphate using Pluronic F68. *Anal. Biochem.* **2020**, *597*, 113681. [CrossRef]
24. Vishnikin, A.B.; Al-Shwaiyat, M.E.A.; Bazel, Y.R.; Andruch, V. Rapid, sensitive and selective spectrophotometric determination of phosphate as an ion associate of 12-molybdophosphate with Astra Phloxine. *Microchim. Acta* **2007**, *159*, 371–378. [CrossRef]
25. Hedjazi, M.; Vishnikin, A.B.; Okovytyy, S.I.; Miekh, Y.V.; Bazel, Y.R. Use of dye aggregation phenomenon for spectrophotometric and SIA-LAV determination of bismuth(III) as a specific ion association complex between tetraiodobismuthate and Astra Phloxine. *J. Mol. Struct.* **2022**, *1251*, 132015. [CrossRef]
26. Hedjazi, M.; Vishnikin, A.B.; Balanenko, A.D. A green spectrophotometric method for determination of drotaverine hydrochloride in pharmaceutical preparations using formation of ion association complex with erythrosine. *J. Chem. Technol.* **2021**, *29*, 467–475. [CrossRef]
27. Bertocchi, F.; Delledonne, A.; Vargas-Nadal, G.; Terenziani, F.; Painelli, A.; Sissa, C. Aggregates of cyanine dyes: When molecular vibrations and electrostatic screening make the difference. *J. Phys. Chem. C* **2023**, *127*, 10185–10196. [CrossRef]
28. Huang, X.-L.; Zhang, J.-Z. Surfactant-sensitized malachite green method for trace determination of orthophosphate in aqueous solution. *Anal. Chim. Acta* **2006**, *580*, 55–67. [CrossRef]
29. Kakalejčíková, S.; Bazel, Y.; Fizer, M. Extraction-less green spectrofluorimetric method for determination of mercury using an Astra Phloxine fluorophore: Comprehensive experimental and theoretical studies. *Spectrochim. Acta A* **2024**, *310*, 123946. [CrossRef]
30. Taniai, T.; Sukegawa, M.; Sakuragawa, A.; Uzawa, A. On-line preconcentration of phosphate onto molybdate form anion exchange column. *Talanta* **2003**, *61*, 905–908. [CrossRef]
31. Oshima, M.; Goto, N.; Susanto, J.P.; Motomizu, S. Determination of phosphate as aggregates of ion associates by light-scattering detection and application to flow injection. *Analyst* **1996**, *121*, 1085–1088. [CrossRef]
32. Skok, A.; Bazel, Y.; Fizer, M. A simple green method for the determination of hydrogen peroxide and Fe(III)/Fe(II) species based on monitoring the decolorization process of polymethine dye using an optical immersion probe. *Chemosensors* **2024**, *12*, 270. [CrossRef]
33. Neumann, R.; Khenkin, A.M. Oxidation of dienes and polyenes. In *The Chemistry of Dienes and Polyenes*; Rappoport, Z., Ed.; John Wiley & Sons: Hoboken, NJ, USA, 1997; Volume 1, pp. 889–926.
34. Belko, N.; Maltanava, H.; Lugovski, A.; Shundalau, M.; Osika, Y.; Smaliakou, A.; Fatykhava, S.; Shabunya, P.; Lamberti, P.; Samtsov, M.; et al. Indotricarbocyanine dyes relevant for photodynamic therapy and their radicals: Substituent effects studied by optical and electrochemical methods. *Dyes Pigm.* **2023**, *216*, 111344. [CrossRef]
35. Kulinich, A.V.; Derevyanko, N.A.; Ishchenko, A.A.; Gusyak, N.B.; Kobasa, I.M.; Romańczyk, P.P.; Kurek, S.S. Structure and redox properties of polymethine dyes: Electrochemical and DFT/TD-DFT study. *Dyes Pigm.* **2019**, *161*, 24–33. [CrossRef]
36. Parton, R.; Lenhard, J. Dimerization reactions of cyanine radical dications. *J. Org. Chem.* **1990**, *55*, 49–57. [CrossRef]
37. Rurack, K.; Spieles, M. Fluorescence quantum yields of a series of red and near-infrared dyes emitting at 600–1000 nm. *Anal. Chem.* **2011**, *83*, 1232–1242. [CrossRef]
38. Balogh, I.S.; Kish, P.P.; Ishchenko, A.A.; Mushkalo, I.L.; Andruch, V. Spectrophotometric study of acid-base properties of cationic cyanine dyes. *J. Anal. Chem. USSR* **1990**, *45*, 481–490.
39. Tóth, J.; Bazel, Y.; Balogh, I. A fully automated system with an optical immersion probe (OIP) for high-precision spectrophotometric measurements. *Talanta* **2021**, *226*, 122185. [CrossRef]

40. Mishra, A.; Behera, R.K.; Behera, P.K.; Mishra, B.K.; Behera, G.B. Cyanines during the 1990s: A Review. *Chem. Rev.* **2000**, *100*, 1973–2011. [CrossRef]
41. Xu, F.; Testoff, T.T.; Wang, L.; Zhou, X. Cause, regulation and utilization of dye aggregation in dye-sensitized solar cells. *Molecules* **2020**, *25*, 4478. [CrossRef]
42. Yuzhakov, V.I. Aggregation of dye molecules and its influence on the spectral luminescent properties of solutions. *Russ. Chem. Rev.* **2007**, *61*, 613–628. [CrossRef]
43. Bricks, J.L.; Slominskii, Y.L.; Panas, I.D.; Demchenko, A.P. Fluorescent J-aggregates of cyanine dyes: Basic research and applications review. *Methods Appl. Fluoresc.* **2018**, *6*, 012001. [CrossRef]
44. Mourot, B.; Jacquemin, D.; Siri, O.; Pascal, S. Coupled polymethine dyes: Six decades of discoveries. *Chem. Rec.* **2024**, *24*, e202400183. [CrossRef]
45. Shapiro, B.I. Aggregates of cyanine dyes: Photographic problems. *Russ. Chem. Rev.* **1994**, *63*, 231–255. [CrossRef]
46. Moreno-Villoslada, I.; Fuenzalida, J.P.; Tripailaf, G.; Araya-Hermosilla, R.; Pizarro, G.S.; Marambio, O.G.; Nishide, H. Comparative study of the self-aggregation of Rhodamine 6G in the presence of poly(sodium 4-styrenesulfonate), poly(n-phenylmaleimide-co-acrylic acid), poly(styrene-alt-maleic acid), and poly(sodium acrylate). *J. Phys. Chem. B* **2010**, *114*, 11983–11992. [CrossRef] [PubMed]
47. Struganova, I.A.; Hazell, M.; Gaitor, J.; Mcnally-Carr, D.; Zivanovic, S. Influence of inorganic salts and bases on the J-Band in the absorption spectra of water solutions of 1,1′-diethyl-2,2′-cyanine Iodide. *J. Phys. Chem. A* **2003**, *107*, 2650–2656. [CrossRef]
48. Heyne, B. Self-assembly of organic dyes in supramolecular aggregates. *Photochem. Photobiol. Sci.* **2016**, *15*, 1103–1114. [CrossRef] [PubMed]
49. Lenhard, J.R.; Hein, B.R. Effects of J-aggregation on the redox levels of a cyanine dye. *J. Phys. Chem.* **1996**, *100*, 17287–17296. [CrossRef]
50. Katoh, T.; Inagaki, Y.; Okazaki, R. Linear and stack oligostreptocyanines. Effects of relative orientation of chromophores on redox potentials of dye aggregates. *Bull. Chem. Soc. Jpn.* **1997**, *70*, 2279–2286. [CrossRef]
51. Kawasaki, M.; Sato, T. Direct voltammetric observation of reversible and irreversible oxidations of two-dimensional J-aggregates of cyanine dye. *J. Phys. Chem. B* **2001**, *105*, 796–803. [CrossRef]
52. Lenhard, J.R.; Cameron, A.D. Electrochemistry and electronic spectra of cyanine dye radicals in acetonitrile. *J. Phys. Chem.* **1993**, *97*, 4916–4925. [CrossRef]
53. Neves, M.S.A.C.; Souto, M.R.S.; Tóth, I.V.; Victal, S.M.A.; Drumond, M.C.; Rangel, A.O.S.S. Spectrophotometric flow system using vanadomolybdophosphate detection chemistry and a liquid waveguide capillary cell for the determination of phosphate with improved sensitivity in surface and ground water samples. *Talanta* **2008**, *77*, 527–532. [CrossRef]
54. Zhai, Q.-Z. Determination of phosphorus by phosphorus molybdenum blue spectrophotometry by bismuth antimony sensitization. *Bull. Chem. Soc. Ethiop.* **2023**, *37*, 1307–1313. [CrossRef]
55. Lin, B.; Xu, J.; Yin, C.; Chen, L.; You, Y.; Hu, L. An ultralight dual-wavelength and dual-beam chemical sensor on small UAV for in-situ determination of phosphate and nitrite in surface water. *Sens. Actuators B* **2022**, *368*, 132235. [CrossRef]
56. Mousareza, P.; Alizadeh, N. Near-infrared photothermal lens as microfluidic analyzer for determination of phosphate in food and biological samples. *Microchem. J.* **2024**, *206*, 111674. [CrossRef]
57. Deng, Z.; Zhang, J.; Su, Z.; Bai, Y.; He, J. Derivatization reaction-based multi-spectroscopic techniques for ultrasensitive and rapid detection of phosphate in food using Nile blue A as probe. *Microchem. J.* **2023**, *185*, 108280. [CrossRef]
58. Knochen, M.; Rodríguez-Silva, J.C.; Silva-Silva, J. Exploitation of reaction mechanisms for sensitivity enhancement in the determination of phosphorus by sequential injection analysis. *Talanta* **2020**, *209*, 120589. [CrossRef]
59. Khongpet, W.; Yanu, P.; Pencharee, S.; Puangpila, C.; Hartwell, S.K.; Lapanantnoppakhun, S.; Yodthongdee, Y.; Paukpol, A.; Jakmunee, J. A compact multi-parameter detection system based on hydrodynamic sequential injection for sensitive determination of phosphate, nitrite, and nitrate in water samples. *Anal. Meth.* **2020**, *12*, 855–864. [CrossRef]
60. Manbohi, A.; Ahmadi, S.H. Portable smartphone-based colorimetric system for simultaneous on-site microfluidic paper-based determination and mapping of phosphate, nitrite and silicate in coastal waters. *Environ. Monit. Assess.* **2022**, *194*, 190. [CrossRef]
61. Deng, Y.; Li, P.; Fang, T.; Jiang, Y.; Chen, J.; Chen, N.; Yuan, D.; Ma, J. Automated determination of dissolved reactive phosphorus at nanomolar to micromolar levels in natural waters using a portable flow analyzer. *Anal. Chem.* **2020**, *92*, 4379–4386. [CrossRef]
62. Zaruba, S.; Oltmanova, V.; Andruch, V. Microextraction by packed sorbent for determination of inorganic analytes: Phosphates determination. *Microchem. J.* **2025**, *210*, 112976. [CrossRef]
63. Kel'ina, S.Y.; Nevinsky, O.G. Indirectly determination of phosphate-ions in waters with the reagent sulfonitrazo DAF. *Methods Objects Chem. Anal.* **2021**, *16*, 147–152. [CrossRef]
64. Snigur, D.; Chebotarev, A.; Bulat, K.; Duboviy, V. Fast room temperature cloud point extraction procedure for spectrophotometric determination of phosphate in water samples. *Anal. Biochem.* **2020**, *597*, 113671. [CrossRef]

65. Timofeeva, I.I.; Kochetkova, M.A.; Dvoinykh, D.D.; Safinskaya, Y.V.; Zubakina, E.A.; Bulatov, A.V. Micellar microextraction with alkyl polyglucosides for the preconcentration and spectrophotometric determination of phosphate ions in aqueous media. *J. Anal. Chem.* **2024**, *79*, 1408–1414. [CrossRef]
66. Zhou, J.; Fei, J.; Zeng, C.; Quan, H.H.; Li, M. Cyclic voltammetric determination of phosphate in tap water via $[Omim]_6Mo_7O_{24}$-carbon paste electrodes. *Chem. Pap.* **2023**, *77*, 5873–5880. [CrossRef]
67. Martynov, L.Y.; Sergeeva, A.S.; Sakharov, K.A.; Shkinev, V.M.; Yashtulov, N.A.; Zaitsev, N.K. Voltammetric determination of phosphates using ion-selective electrode based on organotin ionophore. *Microchem. J.* **2023**, *191*, 108877. [CrossRef]
68. Gonçalves, S.; Alves, V.R.; Perez, S.O.; Ferreira, M.; Daguer, H.; de Oliveira, M.A.L.; Micke, G.A.; Vitali, L. Rapid method for the determination of citrate, phosphate and sulfite in seafood by capillary zone electrophoresis. *Food Chem.* **2020**, *321*, 126705. [CrossRef]
69. Yoshikawa, K.; Kogure, F.; Tsukada, K.; Toyama, T.; Sakuragawa, A.; Nagashima, H. Determination of phosphorus in commercially available milk using ion chromatography with perchloric acid deproteinization. *Anal. Sci.* **2024**, *40*, 1365–1371. [CrossRef]
70. Pytlakowska, K.; Kocot, K.; Hachula, B.; Talik, E. Preconcentration of phosphate ions on graphene oxide decorated with lanthanum oxide from waters followed by energy dispersive X-ray fluorescence spectrometric determination. *Talanta* **2024**, *266*, 124997. [CrossRef]
71. Shao, Y.; Ma, S.; Zhao, X.; Tian, H.; Chen, S.; Dong, D.; Zhou, J. Determination of phosphorus in water using iron hydroxide assisted laser-induced breakdown spectroscopy. *J. Anal. Atom. Spectrom.* **2023**, *38*, 638–641. [CrossRef]


**Disclaimer/Publisher's Note:** The statements, opinions and data contained in all publications are solely those of the individual author(s) and contributor(s) and not of MDPI and/or the editor(s). MDPI and/or the editor(s) disclaim responsibility for any injury to people or property resulting from any ideas, methods, instructions or products referred to in the content.